The Jahangirnagar Review: Part II: Social Sciences, Vol. XLIV, 2020
Printed in June 2021, ISSN 1682-422© Jahangirnagar University

Predicating Land Use/Land Cover Changes for 2050 Using CA-Markov Model and LCM: A Case for Maheshkhali Island, Bangladesh

Tanjinul Hoque Mollah[*]
Munia Tahsin[**]
Nur Mohammad[**]
Md. Rakibul Hasan[**]
Naiem Mollah[**]

Abstract: Satellite imagery is a vital tool to study exclusively spatio-temporal distribution of Land Use and Land Cover (LULC) changes including various socio-ecological concerns such as decadal changes of LULC with anthropogenic activities, relations among physical environment, cultural landscape, and human activities. This study used Maheshkhali Island, Bangladesh as a case study. Besides that, there are five multi-temporal Landsat images were used in this study which acquired in 2001, 2005, 2010, 2015, and 2020 accordingly. Among them, threes are from Landsat 5 Thematic Mapper (TM) and twos are from Landsat 8 Operational Land Imager (OLI). Images were classified into eight classes using the maximum likelihood supervised method. This study explores land change matrix for 2000-2020 and predicts the LULC dynamics for 2050 using CA-Markov chain model and Land Change Modeler (LCM). Hereafter, their accuracy was measured by kappa statistics and overall accuracy methods. Finally, this paper reveals that the pattern of land use land cover has been identified from 2001-2020 and predicted the pattern of change for the next 30 years till 2050. It may help the policymakers to make decisions on future landscape planning and to perceive the present condition of Maheshkhali Island for proper management.

Keywords: LULC, Remote Sensing, Change detection, CA-Markov model, Prediction.

1.0 Introduction

As of late, land use and land cover change based research is used broadly in worldwide for identifying the dynamic processes, land change matrix, and its facts. Land use and land cover are the most common term are used in geospatial analysis. Land cover refers to the biophysical condition of the surface of the earth such as soil, vegetation cover, water bodies, and other physical features (Liping et al., 2018). Whereas land use incorporates the ways that land is used. For instance, agriculture, salt production, built-up area, forestry, etc. There is various popular Change Detection Model which are used worldwide for analyzing the past land use pattern and using the trend to predict about the future. Markov model according to CA Markov is one of the significant models as it functions on Spatio-temporal changes of the landform (Mondal et. al, 2016). In the simulation of landscape changes, the Markov model is widely used for its advancement with GIS and remote sensing (Baker, 1989, Muller and Middleton, 1994). Maheshkhali is the only mountainous island of Bangladesh and it has the unique geologic condition and geomorphologic complexities. The island is unique in this term that Maheshkhali Island

[*] Associate Professor, Department of Geography and Environment, Jahangirnagar University, Savar, Dhaka-1342, Bangladesh. Email: thmollah@juniv.edu
[**] Research Student, Department of Geography and Environment, Jahangirnagar University, Savar, Dhaka-1342, Bangladesh, Email: muniju45@gmail.com, nurmohammadju45@gmail.com, rakibhsumon@gmail.com, mollahniem79@gmail.com

is the type of accretion landform since 1972. From 1972 to 2010 (38 years) it added about 47 sq. km at a rate of 1.2 sq. km per year (Islam, 2011).

Maheshkhali Island and its neighboring area along with Cox's Bazar, Matarbari and Sonadia Island have gone through egregious changes recently because Government wants to make it the digital island with seventeen projects where exist three power plants, four gas pipelines, two LNG terminals, five economic zones, one regional highway, and one eco-tourism park along with an IT park (BWGED, 2017). It can be identified and analyzed by using LULC models and Land Change Modeler (LCM) from Landsat satellite images that help to evaluate land-use policy. The establishment of these development projects will change the pattern LULC of Maheshkhali. The simulation of the spatial pattern of LULC obtained from the probability of transition matrix from Markov and CA Markov helps to predict the future LULC change based on the transition matrix of the past with affecting driving forces (Han et al., 2015; Gillanders et al., 2008). Using kappa statistics, the model is validated and kappa statistics is the best as it counts the pixel-level accuracy (Pontius et al., 2003).

The main concern of the study is to analyze the land use land cover pattern of greater Maheshkhali Island from 2000-2010 and 2010-2020 using Markov and CA Markov along with LCM and from this matrix analysis predict the land use land cover of 2050. Therefore, the main goal of this study is to 1) analyze the land use land cover change of 2000-2020 using Landsat TM and OLI along with Markov and CA Markov 2) predict about the LULC of 2050 using the transition probability matrix trend.

2.0 Data and Method Description

2.1 Study Area

The Maheshkhali Island is the only hilly island which is located in the northwestern part of Cox's Bazar district, Bangladesh lies within 21° 20′ N- 21°50′ N latitude and 91°45′E - 92°00′E longitude separated from the mainland through the Maheshkhali channel.

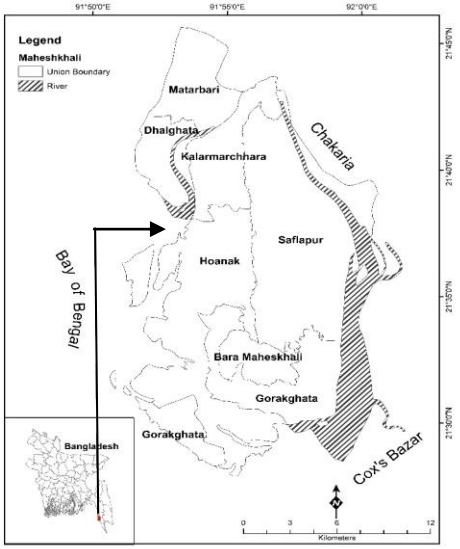

Figure 1: Study Area map of Maheshkhali Island, Cox's Bazar District

Source: Compiled by authors, 2020

The greater Maheshkhali Island which is constituted with Sonadia, Matarbari, and Dhalghata Island where Matarbari Island joint with Dhalghata Island is separated from the Maheshkhali mainland by the Kuhelia River whereas Sonadia situated in the southwestern part separated by Baddar Khal (Majlis, 2013). The study covers an area of approximately 38850 ha. Recently the area has gone through major LULC changes because of rapid developments in every sector planned by the Government.

2.2 Data and Methods and Processing Approaches

Five Landsat images were downloaded from the United States Geological Survey (USGS) which are used in this study. Three Landsat 5 Thematic Mapper (TM) for the analysis of 2000, 2005, 2010, and two Landsat 8 Operational Land Imager (OLI) were downloaded for 2015 and 2020. The image was processed by ERDAS IMAGINE 2014 and IDRISI Selva software.

Table 1: Detail information of satellite images used in this research

Satellite Imagery	**Path/Row**	Acquisition date	Resolution (m)
Landsat 5 Thematic Mapper (TM)	135/045	13/12/2000	30m
Landsat 5 Thematic Mapper (TM)	135/045	25/11/2005	30m
Landsat 5 Thematic Mapper (TM)	135/045	23/11/2010	30m
Landsat 8 Operational Land Imager (OLI)	135/045	23/12/2015	30m
Landsat 8 Operational Land Imager (OLI)	135/045	20/02/2020	30m

Source: Compiled by authors, 2020

Based on our study, each satellite images were classified in 8 classes which are orderly mangrove forest, salt field, hills, homestead vegetation, built-up area, agricultural land, water bodies, and beach which are listed below with their training sample as well as ground control points -

Table 2: Based on LULC each satellite images were following categories

Class	Subclass	Training sample x 9 pixels	Ground Control Points (GCP)
1. Mangrove forest	1.1 Natural Mangrove Forest 1.2 Planted Mangrove Forest	10	4
2. Salt field	2.1 Salt bed	15	9
3. Hills	3.1 Hilly area	9	2
4. Homestead vegetation	4.1 Homestead vegetation 4.2 Plantations	8	7
5. Built up area	5.1 Homestead 5.2 Constructed area	13	11
6. Agricultural land	6.1 Fallow land 6.2 Crop land	7	5

Class	Subclass	Training sample x 9 pixels	Ground Control Points (GCP)
7. Water bodies	7.1 Pond 7.2 Lagoon	22	6
8. Beach	8.1 Tidal zone 8.2 Intertidal zone	5	3

Source: ERDAS IMAGINE® Tour Guides™. (2006). Norcross, Georgia: Leica Geosystems Geospatial Imaging, LLC

Overall classification accuracy was evaluated by a confusion matrix. Besides, the overall accuracy, user's accuracy, producer's accuracy, and kappa statistics are used for the accuracy assessment. As the study is based on both primary and secondary data, the accuracy assessment was verified by the field observation. Not only are those, for better evaluation of the classes which were orderly organized and interpreted here are analyzed by photo-interpretation techniques through Google Earth Pro.

By analyzing the LULC pattern for 2000, 2005, 2010, 2015, 2020 a confusion matrix (8*8) had obtained through Markov analysis. Using the confusion matrix, the probability of changing can be estimated. (Hamad, 2018). From the cross-tabulation matrix combined with the cellular automata and transition probability matrix which is commonly known as CA Markov is used here for predicting the land use land cover of 2050 for Maheshkhali Island based on 2000-2010 matrix and 2010-2020 matrix.

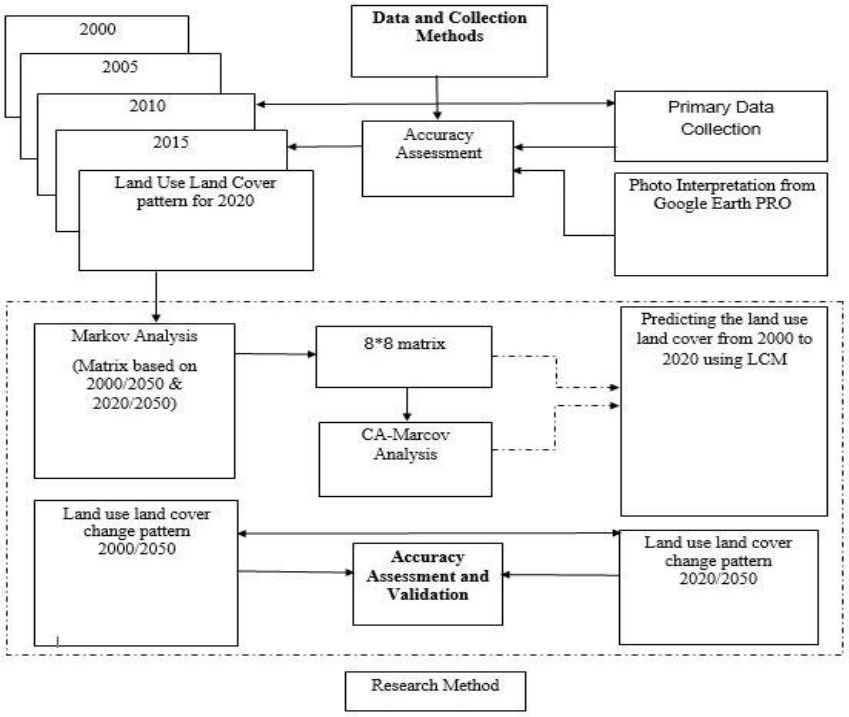

Figure 2: Conceptual framework of the study.

Source: Made by authors, 2020

Here, is the land use land cover distribution map which is acquired from the analysis of Landsat images. Each color represents the distribution of the area of each classified LULC which are for five different periods (2000, 2005, 2010, 2015, 2020).

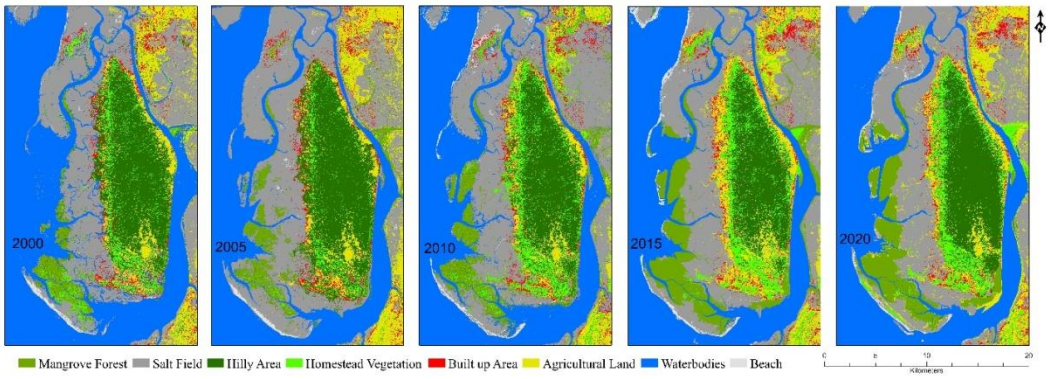

Figure 3: LULC distribution map for Maheshkhali Island of five different periods.

Source: Compiled by authors, 2020

The overall distribution of area for this studied year of Maheshkhali Island is shown in hectares as a data table according to years from where we can analyze the pattern of changes of the LULC over time.

Table 3: Temporal distribution in hectares of each LULC class

LULC	2000	2005	2010	2015	2020
Mangrove Forest	2753.37	2923.16	3534.33	4277.10	4912.83
Salt Field	8380.05	8466.75	8459.91	9574.34	10268.73
Hills	6467.38	6423.39	6429.80	6313.29	6100.92
Homestead Vegetation	1640.78	1926.16	2266.99	1962.14	2071.39
Built-Up Area	1186.11	1428.57	1763.47	1977.28	2187.47
Agricultural Land	5195.72	4971.47	4651.14	4453.72	4238.61
Water Bodies	10182.10	9823.77	9568.82	9377.24	8979.24
Beach	923.13	868.53	651.01	579.7	527.15
Total	36728.64	36831.8	37325.47	38514.81	39286.34

Source: Made by authors, 2020

3.0 LULC Change Analysis using CA-Markov

3.1 The Markov Model of LULC Change

The Markov model is a framework that provides a land-use simulation of inter-temporal land use shifts and analyzes future use of land. Burnham in 1973 first used the model for the southern Mississippi alluvial valley (Burnhum, 1973). In the Markov model, specific land-use patterns are segmented into different classes and they are observed for a specific

time in the past and then summarized in a transition matrix. Using that matrix, it is calculated the probability of shifting for the future time frame which is known as transition probability matrix (Burnhum, 1973).

The calculation of the shifting of the land use change can be calculated through this equation-

$$S\ (t, t+1) = P_{ij} \times S(t)$$

Here, *S* is the system status, *t* is the system status for time initial period and *t+1* is the system status of desired period, and these are calculated like this-

$$= \|p_{ij}\| = \begin{Vmatrix} P_{1,1} & P_{1,2} & \cdots & P_{1,N} \\ P_{2,1} & P_{2,2} & \cdots & P_{2,N} \\ \cdots & \cdots & \cdots & \cdots \\ P_{N,1} & P_{N,2} & \cdots & P_{N,N} \end{Vmatrix}$$

$$(0 \leq P_{ij} \leq 1)$$

P*ij* stands for the probability matrix which is calculated from initial state *i* to desired state *j*. A probability near 0 recommends the low transition where 1 represents the high (Kumar et all. 2014 and Behera et. all 2012).

3.2 The CA Markov-Chain Model (CA-MCM)

There is numerous model to operate analysis of the shifting land use in terms of inter-temporal location, But in the field of land use modeling researches, Cellular Automata is the most common modeling which is able to simulate and predict the changes (Batty and Xie, 1994 and Clarke and Gaydos 1998). A grid of automata only becomes the CA when the state of the neighboring cell defines the set of the input cell (Jamal et. all., 2011).

In the CA-Markov model, the Markov chain helps to analyze inter-temporal land shifting through a two-dimensional probability matrix, and this model is examined through using the three parameters k_{no}, $k_{location}$ and $k_{quantity}$ of kappa statistics (Pontius, R.G 2000). According to Eastman 0.80 is the satisfactory result of future prediction (Eastman, J.R 2006) and if the value is more than 0.80 describes a well-defined simulation.

4.0 Results and Discussion

4.1 Accuracy Assessment

For different LULC class of Maheshkhali island producer's accuracy, user's accuracy is varied for different time period. From the table 4 shows that overall accuracy is 87, where overall kappa statistics is 0.87 respectively.

Table 4: Accuracy assessment of LULC class for different time period

Land Use/Cover	2001		2005		2010		2015		2019	
	P	U	P	U	P	U	P	U	P	U
Mangrove Forest	87	89	83	89	88	89	88	90	89	87
Salt Field	89	87	87	89	88	89	89	88	88	85
Hills	81	87	84	87	81	87	88	88	84	87
Homestead Vegetation	88	88	89	87	90	87	85	83	86	85
Built-Up Area	89	87	87	89	84	86	87	89	89	88
Agricultural Land	83	87	87	88	82	83	81	88	86	87
Water Bodies	85	87	88	87	89	88	89	87	87	85
Beach	87	88	83	88	88	88	88	87	84	89
Overall accuracy	87		87		87		87		87	
Overall Kappa Statistic	0.87		0.87		0.87		0.87		0.87	

Source: Made by authors, 2020

** P= Producer's accuracy and **U= User's accuracy.

4.2 LULC Change Analysis using LCM and CA Markov

All classes in Maheshkhali Island can be analyzed using the summary of the probability matrix and land change modeler. Row categories are characterized by LULC classes in 2000 where column categories characterized the LULC of 2010. The cross-tabulation matrices are represented in table-5 for the changing probability of 2000-2010 and in table-6 for the changing probability of 2010-2020. Deducting the data from the total column of each group achieves the gain whereas deducting the data from the total row for each group achieves the loss.

In the table, the data illustrates that for the specific time period changes took place in all classes which are in the first scenario 2000 to 2010 for 10 years. Here, the probability of remaining mangrove forest to mangrove forest 14.07%, the probability of changing mangrove forest to salt field 17.78%, mangrove forest to hills 17.93%, mangrove forest to built-up area 5.83%, mangrove forest to agricultural land 5.20%, mangrove forest to water bodies 19.90%. So, the probability of loss for its own characteristics of mangrove forest is 85.93% but from the other classes, the probability of gaining the mangrove forest is 83.52%.

Table 5: Transition probability matrix during 2000-2010

Changing from 2000	Probability of Changing by 2010								Subtotals	
	Mang-rove Forest	Salt Field	Hills	H. Veg.	Built-Up Area	Agri. Land	Water Bodies	Beach	Total	Loss
Mangrove Forest	0.1407	0.1778	0.1793	0.1749	0.0583	0.0520	0.1990	0.0180	1.00	0.8593
Salt Field	0.1278	0.1964	0.1052	0.0984	0.0549	0.0413	0.3494	0.0268	1.00	0.8036
Hills	0.1238	0.1721	0.1852	0.1722	0.0705	0.0753	0.1821	0.0189	1.00	0.8184
Homestead Vegetation	0.1353	0.1747	0.1882	0.1876	0.0603	0.0560	0.1807	0.0172	1.00	0.8124
Built-Up Area	0.1001	0.1637	0.1897	0.1543	0.0921	0.1174	0.1608	0.0218	1.00	0.9079
Agricultural Land	0.0968	0.1590	0.1985	0.1583	0.0968	0.1286	0.1415	0.0206	1.00	0.8714
Water Bodies	0.1367	0.1968	0.1031	0.0991	0.0492	0.0320	0.3592	0.0239	1.00	0.6408
Beach	0.1147	0.2087	0.0857	0.0797	0.0574	0.0397	0.3745	0.0396	1.00	0.9604
Total	0.9759	1.4492	1.2349	1.1245	0.5395	0.5423	1.9472	0.1868		
Gain	0.8352	1.2528	1.0497	0.9369	0.9079	0.4137	1.588	0.1472		

Source: Made by authors, 2020

Like the mangrove forest, the probability of remaining salt field to salt field 19.64%, the probability of future changes for the salt field to mangrove forest 12.78%, salt field to hills 10.52%, and salt field to homestead vegetation 9.84%, salt field to built-up area 5.49%, salt field to agricultural land 4.13%, salt field to water bodies 34.94%, salt field to beach 1.80% and so on for the other LULC.

In the second period (2010-2020), the probability of change, for example, the probability of remaining mangrove forest to mangrove forest 5.43%, the probability of changing mangrove forest to salt field 18.76%, mangrove forest to hills 17.54%, mangrove forest to built-up area 5.46%, mangrove forest to homestead vegetation 13.58%, mangrove forest to agricultural land 26.59%, mangrove forest to water bodies 12.04%. So, the probability of loss for its own characteristics of mangrove forest is 94.57% but from the other classes, the probability of gaining the mangrove forest is 34.83%.

Table 6: Transition probability matrix during 2010-2020

Changing from 2010	**Probability of Changing by 2020**								**Subtotals**	
	Mangrove Forest	**Salt Field**	**Hills**	**Homestead Vegetation**	**Built-Up Area**	Agri. Land	Water Bodies	Beach	**Total**	**Loss**
Mangrove Forest	0.0543	0.1876	0.1754	0.1358	0.0546	0.2659	0.1204	0.0060	1.00	0.946
Salt Field	0.0382	0.2256	0.1398	0.1082	0.0629	0.2778	0.1392	0.0083	1.00	0.774
Hills	0.0504	0.1330	0.2823	0.1747	0.0495	0.2843	0.0233	0.0025	1.00	0.492
Homestead Vegetation	0.0471	0.1734	0.2442	0.1728	0.0509	0.2680	0.0394	0.0042	1.00	0.827
Built-Up Area	0.0471	0.1720	0.2158	0.1356	0.0604	0.3204	0.0496	0.0047	1.00	0.939
Agricultural Land	0.0451	0.1224	0.2724	0.1561	0.0556	0.3278	0.0183	0.0022	1.00	0.672
Water Bodies	0.0325	0.1392	0.0545	0.1561	0.0546	0.1654	0.4991	0.0104	1.00	0.500
Beach	0.0336	0.1816	0.0962	0.0744	0.0602	0.2278	0.3166	0.0095	1.00	0.990
Total	0.3483	1.3348	1.4806	1.1137	0.4487	2.1374	1.2059	0.0478		
Gain	0.2940	1.1090	1.1983	0.9409	0.3883	1.8096	0.7068	0.0383		

Source: Made by authors, 2020

The transition probability matrices and transition area matrices are developed for predicting the year 2050 using images of 2000 and 2010 of LULC maps concerning with analyzing the changing pattern of 2000-2020 and another prediction for 2050, analyzing the LULC maps of 2010-2020 using the transition probability matrices and transition area matrices of 2020.

Table 7: Transition probability matrix during 2000-2020

Changing from 2000	**Probability of Changing by 2020**								**Subtotals**	
	Mangrove Forest	Salt Field	Hills	Homestead Vegetation	Built-Up Area	Agri. Land	Water Bodies	Beach	Total	Loss
Mangrove Forest	0.3972	0.1509	0.2289	0.173	0.0104	0.0012	0.0377	0.0007	1	0.6028
Salt Field	0.0494	0.3023	0.0195	0,0436	0.0636	0.0149	0.4538	0.0528	1	0.6977
Hills	0.1033	0.1504	0.3527	0.2189	0.0776	0.0789	0.0172	0.0008	1	0.6473
Homestead Vegetation	0.1347	0.1321	0.2489	0.4505	0.0165	0.0049	0.0122	0.0003	1	0.5495
Built-Up Area	0.0153	0.1121	0.2147	0.0758	0.2892	0.2624	0.0071	0.0234	1	0.7108
Agricultural Land	0.0114	0.069	0.2164	0.0698	0.1715	0.4431	0.0055	0.0132	1	0.5569
Water Bodies	0.1247	0.1891	0.0096	0.0173	0.0229	0.0012	0.6254	0.0098	1	0.3746
Beach	0.0135	0.3628	0.0027	0.0077	0.0582	0.0002	0.2229	0.3321	1	0.6679
Total	0.8495	1.4687	1.2934	1.0566	0.7099	0.8068	1.3818	0.4331	1	
Gain	0.4523	1.1664	0.9407	0.6061	0.4207	0.3637	0.7564	0.101		

Source: Made by authors, 2020

The simulation for 2000-2020 showed that, the probability of remaining mangrove forest to mangrove forest 39.72% where the probability of changing mangrove forest to salt field 15.09%, mangrove forest to hills 22.89%, mangrove forest to built-up area 1.04%, mangrove forest to homestead vegetation 1.73%, mangrove forest to agricultural land 0.12%, mangrove forest to water bodies 3.77%. So, the probability of loss for its characteristics of mangrove forest is 60.28% but from the other classes, the probability of gaining the mangrove forest is 45.23%.

Here, presented two simulations where 2050 is predicted based on the matrix of 2000-2010 and another simulation presented for the matrix of 2010-2020. Maheshkhali Island is the depositional landform (Islam, 2011) for that landform increasing its area every year wherein 2000 it was only 36728.65 hectares and it becomes 39286 hectares in 2020 which presents a clear comparison between the two simulations that matrix of 2000 predicts 44837 hectares for 2050 and another matrix of 2020 predicts 46439 hectares for 2050.

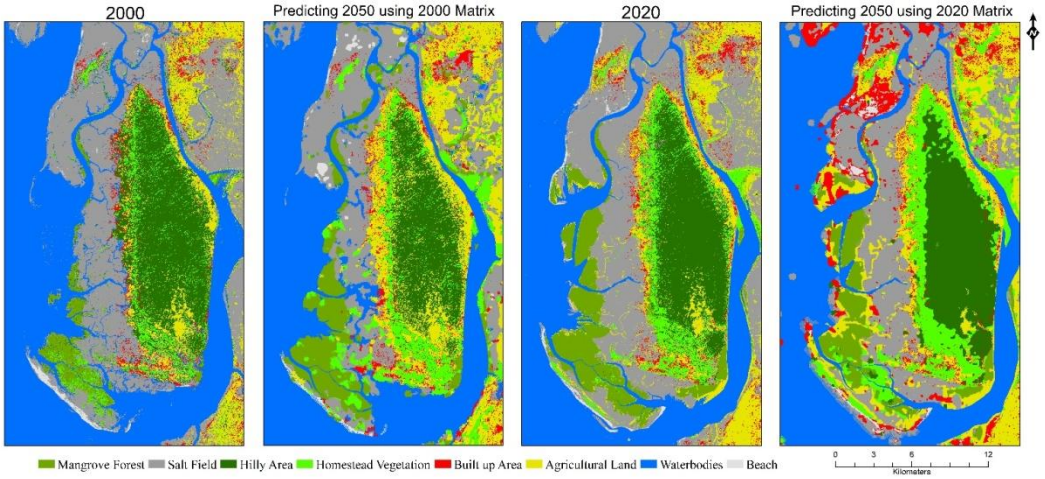

Figure 4: Predicted LULC of Maheshkhali for 2050

Source: Made by authors, 2020

Table 8 illustrates the area statistics for all classes' categories for different periods. From the data the results show that there is a continuous increasing in mangrove forest which supports the accretion characteristics of Maheshkhali.

Salt field cultivation increased slightly from 2000-2020 and then decreased in 2050. Hills are decreasing slightly where in 2000 it was 6467.38 ha, it decreased in 2020 (6100 ha). Homestead vegetation pattern increased over time with the enhancement of built up area and development activities. Agricultural land, water bodies and beach are gradually decreased over time.

Table 8: Area statistics for actual LULC classes for different projected years.

LULC	LULC 2000 (hectares)	LULC 2020 (hectares)	LULC 2000-2050 (hectares)	LULC 2020-2050 (hectares)
Mangrove Forest	2753.37	4912.83	6671.93	6972.87
Salt Field	8380.06	10268.73	7078.76	7363.64
Hills	6467.38	6100.92	4611.23	4711.23
Homestead Vegetation	1640.78	2071.39	5340.89	7140.89
Built-Up Area	1186.11	2187.47	4014.71	8714.71
Agricultural Land	5195.72	4238.615	7798.1	3298.1
Water Bodies	10182.1	8979.24	7913.63	7813.03
Beach	923.13	527.15	1509.03	425.03
Total	36728.65	39286.38	44837.69	46439.50

Source: Made by authors, 2020

4.3 Model Validation

To validate the model**,** there have been drawn up a comparison between actual land use land cover and predicted land use land cover. If K_{IA} values draw up a better comparison between actual land use land cover and predicted land use land cover, it may easily mention that the model is well designed (Hamad et. all., 2018).

Table 9: κ values for 2000 and 2020 to validate the model

4. κ Indicators	2000	2020
κ_{no}	0.8644	0.8935
$\kappa_{location}$	0.8210	0.8007
$\kappa_{locationstrata}$	0.8210	0.8007
$\kappa_{standard}$	0.8200	0.8730

Here, all values are more than 80% which indicates that accuracy assessment was sufficiently accurate. From the statistics, the κ_{no} for 2000 is 0.8644 where it is 0.8935 for 2020. The $\kappa_{location}$ is 0.8210 for 2000 and 0.8007 for 2020. The value of $\kappa_{locationstrata}$ is 0.8210 for 2000 where 0.8007 for 2020. Last, $\kappa_{standard}$ value is 0.8200 for 2000 and 0.8730 for 2020. These all values are more than 80% which provides a good accuracy assessment for this model (Eastman, 2006).

5.0 Conclusion

In recent years, because of development projects accomplished by the Govt. Maheshkhali Island has undergone rapid LULC changes which are clearly sighted in this paper. According to the result of the classification, LULC of the different projected year

displayed that there's an increment of areas of Maheshkhali over time. The overall simulation shows that over time (2000-2020), agricultural land, hills, beach, and water bodies decreased whereas other classes are increased and using the simulation derived from the matrix, showed that in 2050 salt field, hills, beach and water bodies will decrease because of development projects as well as human influence with rapid population growth whereas other classes will increase because of land demands over time. From geographical perspectives as this island has a significant value for its unique morphological characteristics, this study may help the Govt. for planning and management and detect the changes gone through on the island over time.

References

Batty, M. and Xie, Y., 1994. From cells to cities. Environment and planning B: Planning and Design, 21. *Possible Urban Automata*, Pp 31-48. https://doi.org/10.1068/b240175

Baker, R.G., 1989. A review of models of landscape change. Landscape Ecol., 2 (1989), pp. 111-133.

Behera, D.M., Borate, S.N., Panda, S.N., Behera, P.R., Roy, P.S., 2012. Modelling and analyzing the watershed dynamics using Cellular Automata (CA)-Markov model: a geo-information based approach. J. Earth Syst. Sci. 2012, 121, 1011–1024.

Burnham, B.O., 1973. Markov intertemporal land use simulation model. J. Agric. Appl. Econ. 1973, 5, 253–258.

Clarke, K.C. and Gaydos, L.J., 1998. Loose-coupling a cellular automation model and GIS: long-term urban growth prediction for San Francisco and Washington/Baltimore. Geographical Information Sciences, 12(7), 699-714.

Eastman, J.R., 2006. *IDRISI Andes Tutorial*, Clark Labs: Worcester, MA, USA, 2006.

ERDAS IMAGINE® Tour Guides™, 2006. Norcross, Georgia: Leica Geosystems Geospatial Imaging, LLC.

Gillanders, S. N., Coops, N. C., Wulder, M. A., and Goodwin, N. R., 2008. Application of landsat satellite imagery to monitor land-cover changes at the Athabasca Oil Sands, Alberta, Canada. Canadian Geographer, 52(4), 466–485. https://doi.org/10.1111/j.1541-0064.2008.00225.x

Han, H., Yang, C., and Song, J., 2015. Scenario simulation and the prediction of land use and land cover change in Beijing, China. Sustainability (Switzerland), 7(4), 4260–4279. https://doi.org/10.3390/su7044260

Islam, M.A., Majlis A.B.K and Rashid, M.B., 2011. Changing face of Bangladesh coast, The Journal of Noami, Vol.28, Number-1, pp 1-13(June).

Jamal et. al., 2011.Tracking dynamic land-use change using spatially explicit markov chain based on cellular automata: The case of Tehran.

Kumar, S., Radhakrishnan, N., Mathew, S., 2014. Land use change modelling using a markov model and remote sensing. Geomat. Nat. Hazards Risk 2014, 5, 145–156.

Liping, C., Yujun, S., and Saeed, S., 2018. Monitoring and predicting land use and land cover changes using remote sensing and GIS techniques: a case study of a hilly area, Jiangle, China. PLoS ONE, 13(7), 1–23. https://doi.org/10.1371/journal.pone.0200493.

Majlis, A.B.K., Islam, Hossain, Ahsan, 2013. Protected to open basin depositional system: an approach for the Late Quaternary Evolution of the Maheshkhali-Kutubdia Coastal Plain, Bangladesh.

Mondal. S., Sharma, N., Garg, P.K., Kappas, M., 2016. Statistical independence test and validation of CA Markov land use land cover (LULC) prediction results, The Egyptian Journal of Remote Sensing and Space Science, Volume 19, Issue 2, December 2016, Pages 259-272.

Muller, M.R., Middleton, J., 1994. A markov model of land-use change dynamics in the Niagara region, Ontario, Canada, Land-scape Ecol., 9 (2) (1994), pp. 151-157.

Pontius, R.G., 2000. Quantification error versus location error in comparison of categorical maps. Photogramm. Eng. Remote Sens. 2000, 66, 1011–1016.

Pontius, R.G., 2003. Statistical methods to partition effects of quantity and location during comparison of categorical maps at multiple resolutions. Photogram. Eng. Rem. Sens., 68 (10) (2002), pp. 1041-1049.

Rahel, H., Balzter, H., and Kolo, K., 2018. Predicting Land Use/Land Cover Changes Using a CA-Markov Model under Two Different Scenarios.